From experimental investigation to optimized design: A time-efficient methodology for carbon fiber composite crash structures in Formula student applications

Szederkényi B., Bulman V.

Accepted for publication in Periodica Polytechnica-Transportation Engineering
Published in 2025
DOI: https://doi.org/10.3311/PPtr.40303

Periodica Polytechnica Transportation Engineering, 53(4), pp. 446–454, 2025

From Experimental Investigation to Optimized Design: A Time-efficient Methodology for Carbon Fiber Composite Crash Structures in Formula Student Applications

Bence Szederkényi[1*], Vencel Bulman[1,2]

[1] Department of Polymer Engineering, Faculty of Mechanical Engineering, Budapest University of Technology and Economics, Műegyetem rkp. 3., H-1111 Budapest, Hungary
[2] Red Bull Engineering Academy, Red Bull Advanced Technologies, Red Bull Technology Campus, Stewart Building, 1 Bradbourne Drive, Tilbrook, MK7 8BJ Milton Keynes, United Kingdom
* Corresponding author, e-mail: szederkenyib@pt.bme.hu

Received: 08 March 2025, Accepted: 01 July 2025, Published online: 30 July 2025

Abstract

This study presents the design and numerical validation of a composite impact attenuator, with Formula Student serving as a proof of concept. The research methodology involved an initial calibration phase, where simulations of simple test geometries were iteratively refined to match experimental data from dynamic tests within a 1% error margin. These validated material parameters were then applied to a final impact attenuator design featuring a five-tube configuration. To enhance time and cost efficiency, physical testing was conducted only at the intermediate component level, where simulation models were calibrated. The final crash structure was then optimized entirely through virtual simulations, eliminating the need for full-scale physical prototyping. Finite element simulations demonstrated that the proposed structure meets established deceleration and energy dissipation criteria with a significant safety margin. Additionally, compared to a commercially available aluminum honeycomb attenuator, the composite design achieved equivalent energy absorption characteristics while reducing weight by 13%. These findings validate the proposed methodology and highlight the advantages of composite crash structures for high-performance applications.

Keywords

crash box, compression tests, energy absorption, long-fibre composite, cylindrical shell

1 Introduction

Fiber-reinforced polymer (FRP) composites are increasingly replacing metals in aerospace, automotive, and motorsport applications owing to their high strength-to-weight ratio, corrosion resistance, and durability. Typically composed of carbon, glass, or aramid fibers embedded in polymer matrices such as epoxy, polyester, or vinyl ester, these materials offer a unique advantage in crash structures. Unlike metals, which dissipate energy predominantly through plastic deformation, composites absorb energy through fiber fragmentation and matrix crushing – an intrinsic mechanism that enables higher specific energy absorption and significant weight reduction (Farley, 1983; Thornton, 1979).

Composite failure is complex at the most fundamental level, involving interacting mechanisms across multiple scales. At the microscopic scale, failure initiates through fiber fracture, matrix cracking, fiber pullout, and debonding, forming distinct macroscopic crushing modes. Farley and Jones (1992) identified four principal crushing modes – transverse shearing, local buckling, lamina bending, and brittle fracture – that govern the crash behavior of composite structures. Foundational modeling approaches, such as mesoscale methods and advanced phase-field models, have been developed to capture these phenomena (Bui and Hu, 2021; Li et al., 2019).

Building upon these fundamentals, detailed studies have provided critical insights into damage processes. Tan et al. (2018) demonstrated that curing pressure and interfacial properties critically affect intralaminar and interlaminar damage. Further investigations have explored the role of interlaminar cracking and friction in governing these failure modes (Marton and Szebényi, 2025; Tan et al., 2018).

Composite crash structures mitigate impact forces by controlled energy dissipation – a principle central to their

Cite this article as: Szederkényi, B., Bulman, V. (2025) "From Experimental Investigation to Optimized Design: A Time-efficient Methodology for Carbon Fiber Composite Crash Structures in Formula Student Applications", Periodica Polytechnica Transportation Engineering, 53(4), pp. 446–454.
https://doi.org/10.3311/PPtr.40303

design. Experimental studies confirm that carbon-epoxy composites exhibit superior energy absorption compared to glass- or aramid-epoxy systems (Farley, 1983; Thornton, 1979). Casapu et al. (2024) showed that ply-level hybridization can reduce internal damage and residual strain, thereby enhancing overall crashworthiness.

Ply orientation also plays a pivotal role; for instance, Farley (1983) showed through quasi-static tests on [0/±θ] carbon-epoxy tubes (with the 0° direction as the axial orientation) that absorbed energy decreases with increasing θ, while dynamic tests on [0/±θ] carbon-epoxy, aramid-epoxy, and glass-epoxy specimens indicate that energy absorption may increase with larger off-axis angles (Schmueser and Wickliffe, 1987). These findings underscore that the ply orientations in a layup have a considerable effect on the overall energy absorption capability (Farley and Jones, 1992). Máté and Szekrényes (2024) further confirmed that ply orientation and layup configuration strongly influence composite shells' stability.

At the macro scale, geometric design is equally critical. Thin-walled circular tubes are generally the most effective shape for energy absorption, as stress concentrations in square or rectangular cross-sections lead to premature failure (Mamalis et al., 1992; Thornton and Edwards, 1982). Research on alternative geometries – such as conical shells and hourglass profiles – has demonstrated improved stability and enhanced energy absorption efficiency (Mamalis et al., 1997; Palanivelu et al., 2011). Duan et al. (2014) demonstrated that multi-objective structural optimization can increase specific energy absorption by nearly 68% while reducing peak impact force by over 40%.

Integrating an optimized trigger mechanism into the macro-scale design is essential to initiate a controlled, progressive failure mode throughout the deformable region and ensure uniform energy dissipation, with the semi-apical angle of the frusta serving as the key parameter. A study by Mamalis et al. (1991) found that increasing the semi-apical angle reduces energy absorption and causes a shift from stable to unstable collapse around 15–20°.

Loading conditions further affect composite performance. Dynamic collapse typically results in lower energy absorption compared to quasi-static loading, according to Mamalis et al. (1992) and Schmueser and Wickliffe (1987). Farley (1991) found that while matrix properties are strain-rate dependent, brittle fibers remain largely unaffected. High strain rate studies by Zhang et al. (2024) and Perry and Walley (2022) show that dynamic loading significantly increases both tensile and in-plane shear strengths, enhancing energy absorption while also affecting peak impact loads. Kidane et al. (2017) highlighted the variability of shear properties under high strain rates, while Shokrieh and Omidi (2010) developed a dynamic, progressive damage model that integrates strain rate dependency, achieving excellent agreement with experimental results.

The primary goal of this study is to establish a time- and cost-efficient methodology for designing composite impact attenuators by integrating advanced finite element simulations with targeted experimental validation. Rather than relying on extensive full-scale testing, the approach focuses on calibrating material models through intermediate component-level experiments before applying them to the final structure in a purely virtual optimization process. Demonstrated in a Formula Student context as a proof of concept, this methodology ensures accurate, predictive modeling while significantly reducing development time and resource demands. The insights gained are directly applicable to high-performance crash structures, reinforcing the effectiveness of simulation-driven composite design.

2 Methodology

The primary objective in designing a composite energy-absorbing structure is to achieve a stable, controlled collapse while maximizing specific energy absorption. This study follows the same principle, focusing on analyzing the crushing behavior of composite specimens and developing a calibrated material model based on initial tests to accurately capture this behavior for finite element simulations in the design of lightweight crash structures. A trigger mechanism and appropriate layup will assist the stable crushing modes of the tested specimens. Defining material parameters for FEA will include fitting the simulation results to those of the tested specimen. The static properties of the material had previously been determined and will be used for this analysis. Dynamic properties will be adjusted iteratively, refining their value after comparing the simulation results, limiting them to an essential set of parameters to avoid overcomplicating the process. The crushing process was simulated through the axial compression of composite tube specimens. Given its simple geometry, this method is the most widely studied and provides a straightforward

approach to evaluating the energy absorption characteristics of composite materials.

2.1 Used materials and specimen properties

The material used for this study was the T700S standard modulus carbon fiber prepreg from Toray Industries. The material's fiber content is 36% and is paired with an ER450 resin. The notable material properties include a tensile strength of 2,550 MPa, a tensile modulus of 135 GPa, and a compressive strength of 1,470 MPa, according to the manufacturer.

The specimens were composite tubes (Fig. 1) with an inner diameter of 38 mm and a height of 100 mm. A chamfer was placed at the top of the specimen to act as the crushing trigger, enabling the tube's stable crushing by preventing global buckling.

The layup consisted of four 0.3 mm thick T700 UD plies with (90/0/0/90) layer orientations. The 0° direction denotes the axial direction, while 90° represents the hoop direction. The 90° plies are meant to provide stability by constraining the 0° plies, giving the most significant portion of the energy absorption capability of the structure. The proposed layup was laminated onto a cylindrical mandrel, vacuum-bagged, and cured at 120 °C for 90 min under atmospheric external pressure.

All four specimens, including their dimensions and weight, were measured prior to testing. This data is needed to calculate the specific energy absorption (SEA) of the structure. The SEA is the total amount of energy absorbed per unit mass during crushing, often used to evaluate crashworthiness performance.

Fig. 1 The prepared composite tube specimens. The trigger geometry facing upwards with a ~30° semi-apical angle

2.2 Used equipment

The mechanical tests were carried out with a Zwick Z250 (Zwick GmbH and Co. KG, Ulm, Germany) material testing machine with a testing speed range of 0.001 – 600 mm/min and a maximum load of 250 kN. The tests were performed at the maximum capacity of the machine, using a speed of 600 mm/min (10 mm/s) and a 250 kN load cell. Although crash events occur at considerably higher speeds, this velocity was adequate for calibrating the material model, as suggested by a previous study (Garg et al., 2020).

The results were acquired using the Zwick TestXpert II 3.41 software (Zwick/Roell, 2025) and evaluated in Microsoft Excel (Microsoft Corporation, 2025). The specimen was placed on a flat surface and was axially loaded with a flat load applicator. A Keyence VW-9000 (Keyence International, Mechelen, Belgium) with a resolution of 640 px × 480 px and a maximum recording speed of 230,000 fps high-speed camera was used for the monitoring of the measurements.

3 Results of the single-tube test

The crushing process is showcased in Fig. 2 through images taken from the high-speed camera footage. The specimens with the layup (90/0/0/90) all exhibited crushing behavior during loading. A stable collapse was initiated, with the tubes gradually failing without buckling. Fiber splaying is observed along with fragmentation of the 0° plies.

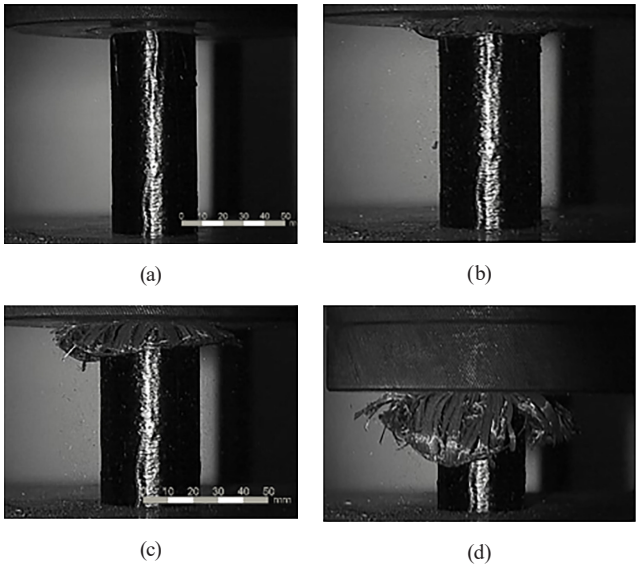

Fig. 2 Crushing process of the composite specimen (a) initial contact stage, showing the intact tubular structure prior to loading, (b) onset of deformation, with visible longitudinal splitting along the tube wall, (c) progressive crushing, characterized by fiber fragmentation and outward splaying, (d) final collapse stage, with extensive frond formation and complete structural failure beneath the platen

4 Numerical simulation

The results of the crushing tests were recreated with numerical simulations to model the crushing characteristics of the material. The defined material properties can later be used to analyze the behavior of complex geometries without the need for physical testing.

4.1 Material models for numerical simulations

The simulation of composite components is carried out using various FE solvers such as ANSYS (ANSYS, Inc., 2025), LS DYNA (Livermore Software Technology Corporation (LSTC), 2025), ABAQUS (Dassault Systèmes, 2025), NASTRAN (MSC Software Corporation, 2025), etc. The current study concerns analyses carried out in LS DYNA with the help of ANSA/ META (BETA CAE Systems, 2025) for pre- and postprocessing, which involves virtually replicating the boundary conditions of physical testing and evaluating the results.

The most important aspect of the analysis is the material model of the CFRP composite material. A good starting point is required to iteratively change the parameters for the results to match those of the physical measurement. Since the simulated crushing process requires a material model with progressive material failure, MAT 54 is commonly used. This material type enables the definition of orthotropic layers in composite shell structures and includes a damage model without excessive complexity. The model is only available within LS DYNA.

A study by Feraboli et al. (2011) using this material model concluded that MAT 54 is suitable for simulating the crushing process in a sinusoidal specimen, albeit through calibration of the parameters by trial and error. The analysis is also susceptible to other parameters such as mesh sizing, contact definition, crush front softening parameter, etc.

4.2 Material parameters

The MAT 54 material card provides many parameters to define both the structure's conventional static behavior and the post-failure mechanisms. The parameters are sorted into groups based on which aspects they control. Numerous parameters are purely mathematical and thus not experimentally definable. These parameters are either damage factors, which reduce various properties of the material following failure, or deletion parameters, which delete an element after reaching the specified value (most often strain). Constitutive and strength properties can be measured experimentally. To simplify the problem, only the parameters with the most significant effect on the crushing behavior were changed during optimization. The modeling of cohesive interface layers between plies was considered but abandoned after several iterations as it complicated the simulation and added too many additional parameters to calibrate.

Longitudinal compressive strength (XC): This parameter was primarily responsible for setting the initial load peak experienced when loading the specimen, with higher values of XC resulting in a higher load peak. It did not have a noticeable influence on the structure's post-crushing behavior.

Maximum strain for fiber tension and compression (DFAILT, DFAILC): These parameters had arguably the most significant impact on the results, as they defined the tensile/ compressive strain at which an element is deleted from the simulation and is no longer able to bear any load.

Low values of the compressive component (DFAILC) lead to global buckling, with the tube failing at the bottom due to premature deletion. Raising the value of this parameter too high leads to insufficient elements being deleted and instability in the simulation. The tensile component plays a vital role in the behavior of the hoop fibers since they are forced inside/outside the structure, with DFAILT as the defining factor for element deletion. Higher values increase the amount of time individual elements remain intact and are able to bear loads.

Maximum strain for matrix tension and compression (DFAILM): This parameter stabilized the simulation. If DFAILT and DFAILC are unsuccessful in deleting enough failed elements, accumulating these distorted elements leads to instabilities and longer simulation run times. DFAILM can delete elements that experience failure in the tensile/compressive matrix direction instead of the fiber direction. Lowering this value could lead to elements being deleted ahead of the crush front or at the bottom of the tube.

Softening reduction factor (SOFT): The SOFT factor defines the "softening" of the stiffness properties of elements at the crush front, which refers to elements neighboring failed (deleted) elements. Its value should be less than 1 and defines the amount by which elements' stiffness properties are multiplied following failure. This function helps avoid high load peaks and buckling due to the sudden loading of the entire tube cross-section.

4.3 Geometry, meshing, boundary conditions, and control parameters

The geometry was a shell tube with a diameter of 38 mm and a height of 100 mm. Using the part card TSHELL_ LAMINATE, a 4-ply laminate with 0.3 mm thick layers was created. The elements were thick shells with a

uniform sizing of 2 mm. The crushing trigger differed from the specimen: the simulation was the most stable when the two outside layers were left an element taller than the inside layers (Fig. 3 (a)).

The loading plate was modeled with a plate placed at the top of the specimen, perpendicular to the axis of the tube. The plate was assigned to the MAT 20 material card, making it a non-deformable rigid body. A constant velocity of 10 mm/s was applied in the axial direction of the specimen according to the calibration tests. The loading plate itself was also the contact, modeled with the CONTACT_ENTITY card, which is a simple but effective contact formulation using a geometric entity instead of a meshed surface. The nodes on the bottom surface of the specimen were constrained in all degrees of freedom to secure the structure (Fig. 3 (b)). The simulations were conducted until the loading plate reached the midpoint of the original specimen height (50 mm). This displacement was sufficient to evaluate the behavior of the tube, as the crushing load had stabilized prior to this point.

4.4 Calibrated material parameters

Below are the results of the iterative parameter definition process. The simulation load curve accurately predicts the mean crushing load and the energy absorbed during the process. The data shown in Fig. 4 was filtered with the 600 Hz SAE method.

To quantify the difference between the simulation and reality, the energy absorption values of the two scenarios were compared. The area under the load-displacement curves was calculated up to 30 mm displacement since all measurements were performed to at least this value. The 30 mm displacement was measured when the reaction force exceeded 1 N. This is necessary because the force

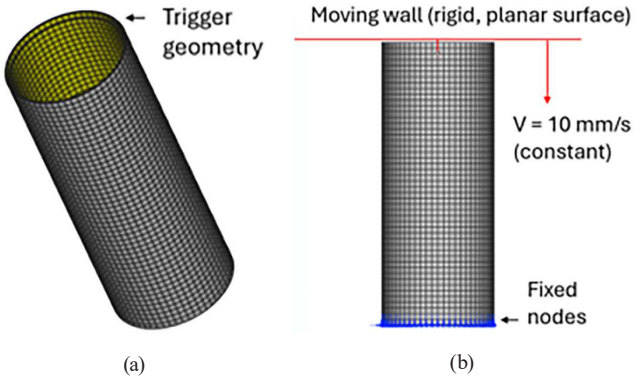

Fig. 3 Simulation model of the calibration tube, showing (a) the trigger geometry oriented outward with its taller elements, and, (b) the applied boundary conditions

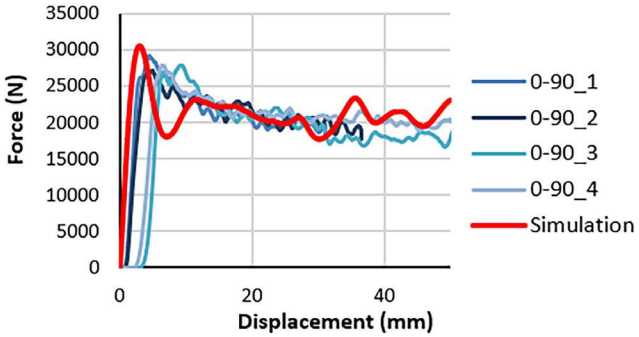

Fig. 4 Load-displacement curves of the measured specimens and the simulation

reaction of the simulation is instantaneous. At the same time, the measurement curves noticeably lag due to the initial gap between the load applicator and the specimen.

The absorbed energy for each measurement and the simulation is displayed in Table 1.

The average energy absorbed during physical testing is 634 ± 11 J, which makes the margin of error between the simulation and reality 1%. Another critical parameter to compare is the peak load, the values of which are also summarized in Table 1.

The average in this case is 28,055 ± 831 N, which means the simulation overestimates reality by 9.2%.

The list of the final material parameters which were iteratively changed during the process is found in Table 2.

In conclusion, the parameters of a simulation model that can accurately predict the absorbed energy of an axially loaded composite tube with negligible deviation from the physical measurement results were defined. This enables the setup of the simulation environment for the crash structure, resulting in layup definition without the need for further physical testing.

5 Design of the crash structure

5.1 Requirements (Formula Student rulebook)

The Formula Student rulebook defines a set of constraints for the design of the crash structure, which can be found under sections T3.17–T3.19 of the rulebook

Table 1 Peak force comparison between the measured specimens and the simulation

Specimen	Absorbed energy (J)	Peak load (N)
0-90_1	644	29,202
0-90_2	641	27,213
0-90_3	619	27,936
0-90_4	631	27,868
Simulation	637	30,629

Table 2 List of final material parameters

Parameter	Value
EA (Young's modulus in 1-direction)	150,000 MPa
EB (Young's modulus in 2-direction)	15,000 MPa
PRBA (minor Poisson's ratio)	0.0192
GAB (shear modulus)	1,200 MPa
XC (compressive strength in 1-direction)	–800 MPa
XT (tensile strength in 1-direction)	2,500 MPa
YC (compressive strength in 2-direction)	300 MPa
YT (tensile strength in 2-direction)	50 MPa
SC (shear strength)	400 MPa
DFAILT (maximum strain for fiber tension)	0.025
DFAILC (maximum strain for fiber compression)	–0.07
DFAILM (maximum matrix tensile/compressive strain)	0.55

(Formula Student Germany, 2022). The main requirements include the energy the structure absorbs (7,350 J) and the geometrical constraints (minimum 200 × 100 × 100 mm). The physical testing conditions on which the simulations are based are also described in detail. The crash structure is referred to as the Impact Attenuator and will be abbreviated as IA from this point forward.

5.2 Geometry and meshing

The selected impact structure consists of a five-tube configuration that complies with the minimum dimension requirements of the regulations. This design was chosen due to its geometric simplicity, ease of manufacturing, and suitability for applying the parameter calibration to simpler geometries. The tube's foremost edges were rounded with a 10 mm radius to direct the fragmented laminate inward, preventing debris accumulation at the crash front and minimizing interactions between components during the design phase. The geometry was discretized using 3 × 3 mm shell elements, as shown in Fig. 5.

5.3 Layup, boundary conditions and control parameters

The final layup of the impact attenuator was determined based on the dimensional constraints, maximum allowable decelerations, the energy absorption requirements specified in the Formula Student regulations, and the reference mass of 385 g for a commercially available aluminum attenuator. To ensure compliance with all these parameters, the selected layup closely followed that of the tested tube specimens, employing a (90/0/0/90) stacking sequence with a reduced ply thickness of 0.25 mm. This resulted in a total wall thickness of 1 mm and an overall mass of 335 g, achieving an approximate 13% weight reduction compared to the aluminum reference.

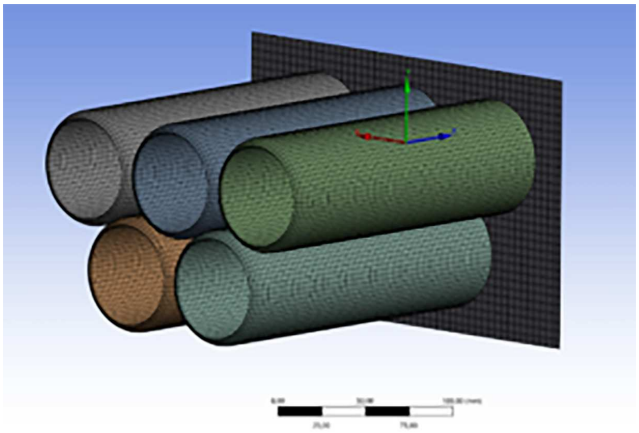

Fig. 5 Meshed geometry of the IA with the inward rounded frontal trigger geometry

All nodes of the surface on which the IA is attached to the car's chassis were constrained in all degrees of freedom. The RIGIDWALL card found in LS DYNA was responsible for loading the structure. This card assigns mass and initial velocity to a plane wall, which will impact the IA. A mass of 300 kg and an initial velocity of 7 m/s were applied to the rigid wall in accordance with FS rules. The runtime of the simulation was defined based on previous drop-tower tests conducted with an aluminum honeycomb energy-absorbing structure, which is the most commonly used in Formula Student. The time to decelerate the mass was about 0.04 s, so a value of 0.06 s was chosen as the termination time.

5.4 Simulation results and discussion

The 10 mm front edge blend applied to the energy-absorbing tubes effectively directed the fragmented laminate into the tube interiors, as shown in Fig. 6. Out of the 200 mm impact zone, 140 mm was entirely crushed to dissipate the initial 7,350 J kinetic energy, leaving a sufficient safety margin for higher-energy impacts and adequate space for debris accumulation.

The parameters to be evaluated are the absorbed energy and mass deceleration plotted as a function of time. These results are presented in Fig. 7.

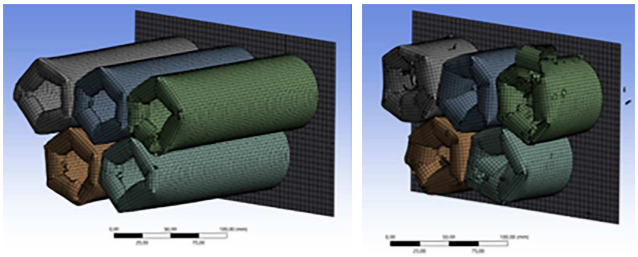

(a) (b)

Fig. 6 The loading phase initiation (a) initial configuration of the composite tube assembly at the start of loading, (b) final equilibrium state after full absorption of kinetic energy

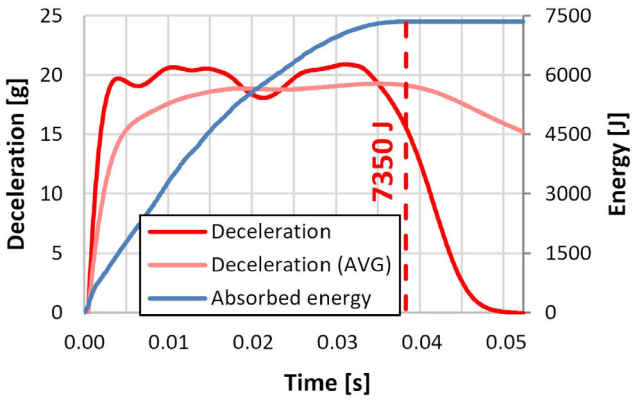

Fig. 7 The absorbed kinetic energy, deceleration, and average deceleration values as a function of time. The red dashed line indicates the point at which the system fully absorbs the imparted kinetic energy

The regulations specify a minimum required energy absorption and impose limits on the peak and average deceleration of the mass as a safety measure to protect the occupant in the event of a crash. The maximum allowable deceleration is 40 g, while the average is limited to 20 g. According to the simulation results, the structure's failure led to a peak deceleration of 21 g and an average deceleration of 13 g. The impact attenuator absorbed 7,350 J of kinetic energy within 0.0377 s, with a deformation of ~140 mm.

6 Conclusions

Fiber fragmentation is the most effective energy absorption mechanism in composites, and it occurs during properly initiated progressive crushing. A well-designed composite structure can absorb more energy per unit mass than its metallic counterpart. In addition to geometry and material properties, the effectiveness of energy absorption also depends on the controlled initiation of the crushing process, a critical design parameter requiring special attention.

The objective of this study was to establish the design criteria for a frontal crash structure. The first phase involved replicating experimental measurements of simple specimen geometries within a simulation framework, followed by iterative calibration of material parameters to match the experimental results. Using the optimized parameters, the simulation results achieved an accuracy within 1% of the measured values. The final stage of the design process focused on defining the geometry and layup of the impact attenuator in compliance with Formula Student regulations. Based on the experimental findings, the initially tested single-tube geometry was modified and multiplied to form a five-tube system. This configuration incorporated an inward-facing trigger mechanism to direct the resulting debris away from the crash front.

According to the simulation results, the final design met the maximum and average deceleration limits prescribed by Formula Student regulations with an approximately twofold safety margin. Compared to the commercially available aluminum honeycomb impact attenuator used as a reference, the proposed composite structure achieved an equivalent energy absorption capacity while reducing mass by 13%.

The prediction and characterization of the crush behavior of composites could be improved by several means. First, a different material model within LS DYNA with more detailed degradation and failure characteristics (e.g., continuum damage models) could yield more accurate results. This would also require extensive material testing. Furthermore, conducting tests with multiple load cases, e.g., off-axis impact and drop tower testing, could provide a better picture of material characteristics outside of quasi-static axial crushing. Actual structures are often subjected to multi-axial loading, which necessitates the characterization of the material properties under these circumstances.

Acknowledgments

The research reported in this paper was supported by the National Research, Development, and Innovation Office (NRDI, Hungary) through grants OTKA K 146236 and OTKA K 138472.

The authors acknowledge the Ministry of Culture and Innovation of Hungary for support from the National Research, Development and Innovation Fund through grant no. NKKP ADVANCED 149578.

Project no. TKP-6-6/PALY-2021 has been implemented with the support provided by the Ministry of Culture

and Innovation of Hungary from the National Research, Development and Innovation Fund, financed under the TKP2021-NVA funding scheme.

The project 2022-2.1.1-NL-2022-00012 has been implemented with the support provided by the Ministry of Culture and Innovation of Hungary from the National Research, Development and Innovation Fund, financed under the 2022-2.1.1-NL Creation of National Laboratories, Complex Development funding scheme.

Bence Szederkényi expresses appreciation for the support of the Doctoral Excellence Fellowship Programme (DKÖP-23-1-BME-64) and of the University Research Fellowship Programme (EKÖP-24-3-BME-419) funded by the National Research Development and Innovation Fund of the Ministry of Culture and Innovation and the Budapest University of Technology and Economics, under a grant agreement with the National Research, Development and Innovation Office.

References

ANSYS, Inc. "ANSYS Mechanical, (Version 2024 R1)", [computer program] Available at: https://www.ansys.com/products/structures/ansys-mechanical [Accessed: 30 June 2025]

BETA CAE Systems "ANSA / META, (Version 24.1.0)", [computer program] Available at: https://www.beta-cae.com/ansa.htm [Accessed: 30 June 2025]

Bui, T. Q., Hu, X. (2021) "A review of phase-field models, fundamentals and their applications to composite laminates", Engineering Fracture Mechanics, 248, 107705. https://doi.org/10.1016/j.engfracmech.2021.107705

Casapu, M., Fuiorea, I., Arrigoni, M. (2024) "Damage assessment through cyclic load-unload tensile tests for ply-level hybrid carbon fiber composites", Express Polymer Letters, 18(1), pp. 41–60. https://doi.org/10.3144/expresspolymlett.2024.4

Dassault Systèmes "Abaqus Unified FEA, (Version 2024)", [computer program] Available at: https://www.3ds.com/products-services/simulia/products/abaqus [Accessed: 30 June 2025]

Duan, S., Tao, Y., Han, X., Yang, X., Hou, S., Hu, Z. (2014) "Investigation on structure optimization of crashworthiness of fiber reinforced polymers materials", Composites Part B: Engineering, 60, pp. 471–478. https://doi.org/10.1016/j.compositesb.2013.12.062

Farley, G. L. (1983) "Energy absorption of composite materials", Journal of Composite Materials, 17(3), pp. 267–279. https://doi.org/10.1177/002199838301700307

Farley, G. L. (1991) "The effects of crushing speed on the energy-absorption capability of composite tubes", Journal of Composite Materials, 25(10), pp. 1314–1329. https://doi.org/10.1177/002199839102501004

Farley, G. L., Jones, R. M. (1992) "Crushing characteristics of continuous fiber-reinforced composite tubes", Journal of Composite Materials, 26(1), pp. 37–50. https://doi.org/10.1177/002199839202600103

Feraboli, P., Wade, B., Deleo, F., Rassaian, M., Higgins, M., Byar, A. (2011) "LS-DYNA MAT54 modeling of the axial crushing of a composite tape sinusoidal specimen", Composites Part A: Applied Science and Manufacturing, 42(11), pp. 1809–1825. https://doi.org/10.1016/j.compositesa.2011.08.004

Formula Student Germany (2022) "Formula student rules 2023", [pdf] Formula Student Germany, Bad Abbach, Germany. Available at: https://www.formulastudent.de/fileadmin/user_upload/all/2023/rules/FS-Rules_2023_v1.0.pdf [Accessed: 10 November 2024]

Garg, R., Babaei, I., Paolino, D. S., Vigna, L., Cascone, L., Calzolari, A., Galizia, G., Belingardi, G. (2020) "Predicting composite component behavior using element level crashworthiness tests, finite element analysis and automated parametric identification", Materials, 13(20), 4501. https://doi.org/10.3390/ma13204501

Kidane, A., Gowtham, H. L., Naik, N. K. (2017) "Strain rate effects in polymer matrix composites under shear loading: A critical review", Journal of Dynamic Behavior of Materials, 3(1), pp. 110–132. https://doi.org/10.1007/s40870-017-0098-2

Li, X., Ma, D., Liu, H., Tan, W., Gong, X., Zhang, C., Li, Y. (2019) "Assessment of failure criteria and damage evolution methods for composite laminates under low-velocity impact", Composite Structures, 207, pp. 727–739. https://doi.org/10.1016/j.compstruct.2018.09.093

Livermore Software Technology Corporation (LSTC) "LS-DYNA, (Version R13.1.0)", [computer program] Available at: https://www.lstc.com/products/ls-dyna [Accessed: 30 June 2025]

Mamalis, A. G., Manolakos, D. E., Demosthenous, G. A., Ioannidis, M. B. (1997) "The static and dynamic axial crumbling of thin-walled fibreglass composite square tubes", Composites Part B: Engineering, 28(4), pp. 439–451. https://doi.org/10.1016/S1359-8368(96)00066-2

Mamalis, A. G., Manolakos, D. E., Viegelahn, G. L., Demosthenous, G. A., Yap, S. M. (1991) "Microscopic failure of thin-walled fibre-reinforced composite frusta under static axial collapse", International Journal of Vehicle Design, 12(5–6), pp. 557–578.

Mamalis, A. G., Yuan, Y. B., Viegelahn, G. L. (1992) "Collapse of thin-wall composite sections subjected to high speed axial loading", International Journal of Vehicle Design, 13(5–6), pp. 564–579. https://doi.org/10.1504/IJVD.1992.061748

Marton, G. Z., Szebényi, G. (2025) "Influencing the damage process and failure behaviour of polymer composites – A short review", Express Polymer Letters, 19(2), pp. 140–160. https://doi.org/10.3144/expresspolymlett.2025.11

Máté, P., Szekrényes, A. (2024) "The effect of the layup on the stability of composite cylindrical shells", Periodica Polytechnica Mechanical Engineering, 68(4), pp. 291–303. https://doi.org/10.3311/PPme.23424

Microsoft Corporation "Microsoft Excel, (Version 2406 Build 17726.20130)", [computer program] Available at: https://www.microsoft.com/en-us/microsoft-365/excel [Accessed: 30 June 2025]

MSC Software Corporation "MSC Nastran, (Version 2024.0)", [computer program] Available at: https://www.mscsoftware.com/product/msc-nastran [Accessed: 30 June 2025]

Palanivelu, S., Paepegem, W. V., Degrieck, J., Vantomme, J., Kakogiannis, D., Ackeren, J. V., Hemelrijck, D. V., Wastiels, J. (2011) "Crushing and energy absorption performance of different geometrical shapes of small-scale glass/polyester composite tubes under quasi-static loading conditions", Composite Structures, 93(2), pp. 992–1007. https://doi.org/10.1016/j.compstruct.2010.06.021

Perry, J. I., Walley, S. M. (2022) "Measuring the effect of strain rate on deformation and damage in fibre-reinforced composites: A review", Journal of Dynamic Behavior of Materials, 8(2), pp. 178–213. https://doi.org/10.1007/s40870-022-00331-0

Schmueser, D. W., Wickliffe, L. E. (1987) "Impact energy absorption of continuous fiber composite tubes", Journal of Engineering Materials and Technology, ASME, 109(1), pp. 72–77. https://doi.org/10.1115/1.3225937

Shokrieh, M. M., Omidi, M. J. (2010) "Dynamic progressive damage modeling of fiber-reinforced composites under different strain rates", Journal of Composite Materials, 44(23), pp. 2723–2745. https://doi.org/10.1177/0021998310369582

Tan, W., Naya, F., Yang, L., Chang, T., Falzon, B. G., Zhan, L., Molina-Aldareguía, J. M., González, C., Llorca, J. (2018) "The role of interfacial properties on the intralaminar and interlaminar damage behaviour of unidirectional composite laminates: Experimental characterization and multiscale modelling", Composites Part B: Engineering, 138, pp. 206–221. https://doi.org/10.1016/j.compositesb.2017.11.043

Thornton, P. H. (1979) "Energy absorption in composite structures", Journal of Composite Materials, 13(3), pp. 247–262. https://doi.org/10.1177/002199837901300308

Thornton, P. H., Edwards, P. J. (1982) "Energy absorption in composite tubes", Journal of Composite Materials, 16(6), pp. 521–545. https://doi.org/10.1177/002199838201600606

Zhang, N., Qian, X., Zhang, Q., Zhou, G., Xuan, S., Wang, X., Cai, D. (2024) "On strain rate effect and high-velocity impact behavior of carbon fiber reinforced laminated composites", Thin-Walled Structures, 194, 111328. https://doi.org/10.1016/j.tws.2023.111328

Zwick/Roell "testXpert, (II 3.41)", [computer program] Available at: https://www.zwickroell.com/services/software-services/ [Accessed: 30 June 2025]